

Ba₂P₈W₃₂O₁₁₂: Structural Study in Comparison with the K and Rb Diphosphate Tungsten Bronzes with Hexagonal Tunnels

M. LAMIRE, PH. LABBÉ, M. GOREAUD, AND B. RAVEAU

*Laboratoire de Cristallographie, Chimie et Physique des Solides, U.A. 251
ISMRA, Université, 14032 Caen Cédex, France*

Received September 15, 1986; in revised form February 10, 1987

The crystal structure of Ba₂P₈W₃₂O₁₁₂ has been solved by three-dimensional single-crystal X-ray analysis. The refinements in the cell of symmetry *A2/m*, with $a = 17.910(2)$ Å, $b = 7.480(2)$ Å, $c = 17.0606(9)$ Å, and $\beta = 114.739(6)^\circ$, has led to $R = 0.038$ and $R_w = 0.045$ for 2194 reflections with $\sigma(I)/I \leq 0.333$. This bronze is the eighth member of the diphosphate tungsten bronze series (DPTB_h) of the general formula $A_x(P_2O_4)_2(WO_3)_{2m}$. A comparison with univalent *A* ion members is made especially for unexplained crystallographic features. A possible interpretation of the observed anomalies deals with the existence of microdomains. © 1987 Academic Press, Inc.

Introduction

During the investigation of the systems *A-P-W-O* (*A* = K, Rb, Tl), a large family of oxides called diphosphate tungsten bronzes, $A_x(P_2O_4)_2(WO_3)_{2m}$, or DPTB_h, was studied (1-5). The main structural features which characterize these structures are now well established: The host framework of these oxides is built up from ReO_3 -type slabs which are *m*-octahedra wide and connected through "planes" of P_2O_7 groups. At the junction of the diphosphate groups and the WO_6 octahedra, hexagonal tunnels are formed where the *A* ions are located.

It is worth pointing out that in these structures several crystallographic features have not been completely elucidated and their origins have not been interpreted up to the present. One important point deals with the existence of superstructures, and also different space groups, correlated with the

splitting of oxygen atoms observed by single-crystal analysis. This problem was interpreted in terms of tilting and distortion of the WO_6 octahedra. In this respect, the recent high-resolution electron microscopy study of the barium diphosphate tungsten bronzes (6) suggests that the nature of the *A* ion may play an important part in these crystallographic problems. For the same *m* value, the barium compounds $Ba_x(P_2O_4)_2(WO_3)_{2m}$ often exhibit a space group different from that of the univalent DPTB_h's; moreover, for these oxides, the superstructure reflections are much more numerous so that the structure cannot be determined on the basis of the subcell, but must be determined in the actual cell.

Thus, the single-crystal X-ray diffraction study of barium DPTB_h's appears as very important in order to understand the structural behavior of these bronzes. This paper deals with the bronze Ba₂P₈W₃₂O₁₁₂, the

eighth member of the DPTB_n series, studied from a single crystal, and analyzes the structural differences between the K, Rb, and Ba compounds.

Experimental

Sample preparation. Mixtures of (NH₄)₂HPO₄, BaCO₃, and WO₃ in appropriate ratios were first heated in air at 873 K to decompose the phosphate and the carbonate. The resultant products were mixed with a suitable amount of metallic tungsten and heated in evacuated silica ampoules for several days at 1473 K, then slowly cooled in air.

Determination of the structure. The crystal selected for the structure determination was a plate limited by {100}, {010}, {001}, and {10 $\bar{2}$ } with dimensions 20 × 72 × 144 μm. The Laue patterns showed a monoclinic symmetry and the Weissenberg technique gave the condition of existence hkl ($k + l = 2n$) involving an A cell.

The intensities of 4767 reflections were collected up to $\theta = 42^\circ$ with a Enraf-Nonius CAD-4 diffractometer, using MoK α radiation (0.71069 Å). The ω - θ technique was used with a scan width of $(1 + 0.35 \tan\theta)^\circ$ and a counter aperture of 1 mm. The background was measured on both sides of each reflection and periodic controls verified the stability of the crystal.

Only 2194 reflections had $\sigma(I)/I \leq 0.333$. These were corrected for Lorentz and polarization effects, then for absorption with a program based on crystal morphology. The minimum and maximum transmission factors were 0.042 and 0.434 ($\mu = 480.9 \text{ cm}^{-1}$). At least-squares refinement based on 25 reflections confirmed the values of the parameters $a = 17.910(2) \text{ \AA}$, $b = 7.480(2) \text{ \AA}$, $c = 17.0606(9) \text{ \AA}$, $\beta = 114.739(6)^\circ$. The structure was solved by the heavy-atom method in $A2/m$.

The data contained 200 measured reflections ($\sigma(I)/I \leq 0.333$) with odd k and there-

fore odd l . These reflections have a weak intensity: the strongest one is 1.1% of the maximum intensity found in the whole spectrum. However, this phenomenon is a new feature observed in the DPTB_n's since only 4 and 7 of such reflections had been significantly measured for Rb_xP₈W₃₂O₁₁₂ (1) and Rb_xP₈W₂₄O₈₈ (2), respectively. It suggests that, for the Ba compound, not only P and O atoms are involved in the process, but also Ba and the W atoms whose positions are slightly distant from the $y = \frac{1}{4}$ and $y = \frac{3}{4}$ planes.

All of the W atom positions were fixed by the Patterson function and refined by least squares. Ba, P, and O were located in the subsequent difference synthesis. Maps of electron density revealed a splitting in the [010] direction for the O atoms out of the $y = 0$ mirror plane due to the fact that the heavy W atoms create a false-mirror plane at $y = 0.25$. The choice of the position for each O atom had to be done by considering the O-O distances: usual O-O distances are about 2.5 Å in PO₄ tetrahedra and 2.7 Å in WO₆ octahedra. The starting point in the structure is the O(4) atom, i.e., the bridging atom in the P₂O₇ group. This operating process led to a unique model, then a general refinement was carried out. Scattering factors for W⁶⁺, Ba²⁺, P, and O²⁻ and anomalous dispersion factors were from the International Tables (7). A linear weighting scheme was adjusted in terms of $\sin \theta/\lambda$. The results (Tables I and II) led to conventional $R = 0.038$ and $R_w = 0.045$.

The corresponding projection of the atomic positions on (010) is drawn in Fig. 1. The case of the bridging O(4) atom whose thermal agitation factor is unusual is discussed elsewhere.

Description of the Structure and Discussion

The host framework of Ba₂P₈W₃₂O₁₁₂ is rather similar to the one of Rb_{1.6}P₈W₃₂O₁₁₂

TABLE I
POSITIONAL AND THERMAL PARAMETERS WITH
e.s.d.'s FOR $\text{Ba}_2\text{P}_8\text{W}_{32}\text{O}_{112}$ (THE CENTER OF
SYMMETRY IS AT THE ORIGIN)

	x	y	z	B (\AA^2)
Ba	$\frac{1}{2}$	$\frac{1}{2}$	$\frac{1}{2}$	$B_{\text{eq}} = 2.0(1)^a$
W(1)	0.25747(3)	0.2491(2)	0.35697(4)	$B_{\text{eq}} = 0.25(1)^a$
W(2)	0.35709(4)	0.2477(3)	0.60271(4)	$B_{\text{eq}} = 0.38(2)^a$
W(3)	0.14923(4)	0.2509(2)	0.61269(4)	$B_{\text{eq}} = 0.28(1)^a$
W(4)	0.05191(4)	0.2505(2)	0.37058(5)	$B_{\text{eq}} = 0.33(1)^a$
P	0.4346(3)	0.2020(7)	0.3261(3)	0.36(6)
O(1)	0.2605(8)	0.230(3)	0.6063(9)	0.7(2)
O(2A)	0.271(2)	0	0.357(2)	1.2(4)
O(2B)	0.279(2)	$\frac{1}{2}$	0.383(2)	1.6(5)
O(3A)	0.055(3)	$\frac{1}{2}$	0.361(3)	2.6(8)
O(3B)	0.056(2)	0	0.381(2)	0.9(4)
O(4)	0.432(4)	0	0.342(4)	5.1(1) ^b
O(5)	0.4791(8)	0.224(2)	0.1151(9)	0.5(2)
O(6)	0.1638(8)	0.234(3)	0.3700(9)	0.8(2)
O(7)	0.326(1)	0.228(3)	0.490(1)	1.5(3)
O(8A)	0.169(2)	0	0.131(2)	0.9(4)
O(8B)	0.150(2)	$\frac{1}{2}$	0.110(2)	0.7(3)
O(9A)	0.362(2)	$\frac{1}{2}$	0.602(2)	1.4(5)
O(9B)	0.382(2)	0	0.626(2)	1.2(4)
O(10)	0.0525(8)	0.233(3)	0.1247(9)	0.7(2)
O(11)	0.3772(9)	0.285(2)	0.362(1)	0.8(2)
O(12)	0.2152(9)	0.277(2)	0.243(1)	0.9(2)
O(13)	0.413(1)	0.216(3)	0.236(1)	1.3(3)
O(14)	0.103(1)	0.281(2)	0.495(1)	0.9(2)
O(15)	0	$\frac{1}{2}$	$\frac{1}{2}$	1.9(4)

^a $B_{\text{eq}} = \frac{1}{3} \sum_i \sum_j \beta_{ij} a_i a_j$

^b See text.

(I) in spite of its different space group. It is built up from the ReO_3 -type slabs which are eight octahedra wide along about the [102]

TABLE II
VALUES OF THE ANISOTROPIC THERMAL
COEFFICIENTS (\AA^2) OBTAINED FROM
 $U_{ij} = (1/2\pi^2) \beta_{ij} a_i a_j$

	U_{11}	U_{22}	U_{33}	U_{12}	U_{13}	U_{23}
Ba	0.071(3)	0.008(1)	0.016(2)	0.0	0.022(2)	0.0
W(1)	0.0038(2)	0.0040(2)	0.0040(3)	-0.0016(9)	0.0026(2)	0.0001(7)
W(2)	0.0035(2)	0.0099(3)	0.0029(3)	-0.001(1)	0.0021(2)	-0.0013(8)
W(3)	0.0054(2)	0.0027(2)	0.0058(3)	-0.001(1)	0.0037(2)	0.0004(7)
W(4)	0.0067(2)	0.0023(2)	0.0076(3)	0.000(1)	0.0048(2)	0.0000(8)

direction, connected through "planes" of diphosphate groups (Fig. 1). It is worth noting that, in the tunnels running along [010], the $2(c)$ positions $\frac{1}{2} \frac{1}{2} \frac{1}{2}$ are fully occupied by the barium ions.

The interatomic W-O, P-O, and Ba-O distances, listed in Table III, allow the geometry of polyhedra to be compared. The structure is built from three sorts of octahedra: W(3)O₆ and W(4)O₆ are surrounded only by WO₆ octahedra whereas W(1)O₆ is linked to five octahedra and one PO₄ tetrahedron. The third type is W(2)O₆ which shares its corners with four WO₆ and two PO₄. The values of the Table III confirm the influence of the P atoms on the localization of W inside its octahedron. The tendency to

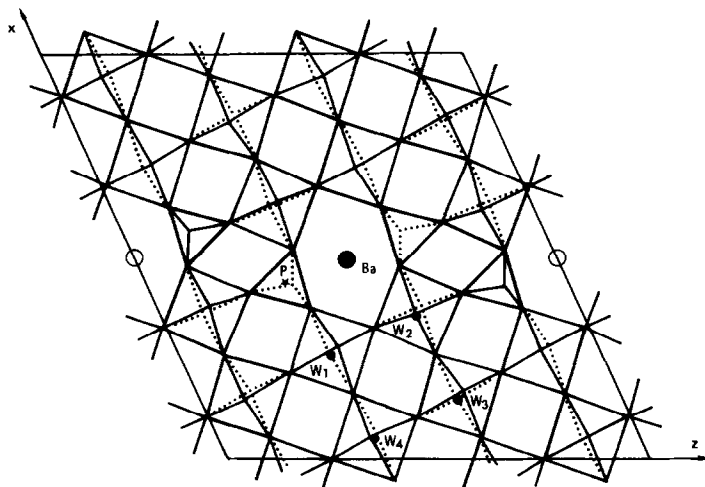


FIG. 1. Projection of the structure onto (010) limited from $y = 0$ to $y = \frac{1}{2}$.

TABLE III
COORDINATION OF Ba, P, AND W ATOMS IN
 $\text{Ba}_2\text{P}_8\text{W}_{32}\text{O}_{112}$ (INTERATOMIC DISTANCES
ARE GIVEN IN Å)

	Ba	P	W(1)	W(2)	W(3)	W(4)
O(1)				1.76(2)	2.05(2)	
O(2A)			1.879(5)			
O(2B)			1.929(7)			
O(3A)						1.876(6)
O(3B)						1.881(3)
O(4)		1.54(2)				
O(5)	4 × 2.72(2)	1.55(1)		2.12(1)		
O(6)			1.78(2)			2.01(2)
O(7)			2.09(2)	1.77(2)		
O(8A)					1.898(5)	
O(8B)					1.878(2)	
O(9A)					1.890(3)	
O(9B)					1.908(6)	
O(10)					1.83(2)	1.91(2)
O(11)	4 × 2.94(1)	1.53(2)	2.12(2)			
O(12)			1.78(2)		2.05(1)	
O(13)		1.43(2)		2.08(2)		
O(14)					1.84(2)	1.94(2)
O(15)						1.8696(7)

a 4 + 2 coordination for W is more apparent if the number of PO_4 linked to the WO_6 octahedron increases. The distance of W from the center of gravity of the oxygen atoms forming the octahedron is 0.05(1) and 0.15(2) Å for W(4) and W(3), respectively, whereas it is 0.23(2) and 0.25(2) for W(2) and W(1). The values observed in $\text{Rb}_{1.6}\text{P}_8\text{W}_{32}\text{O}_{112}$ (1) for the same sorts of W atoms, i.e., 0., 0.14(2), 0.24(2), and 0.24(2) Å, are almost identical to those of the Ba member.

It is known that the distortion of WO_6 octahedra is related to the oxidation state of the W atoms (8, 9). The calculation of the valence v_w of the atoms is made from the relation $v = (R_0/R)^n$ where $n = 5.75$ is based on a characteristic value for W, $R_0 = 1.881$ is the mean length of W–O bonds in the structure, and R is the interatomic W–O distance. The results are given Table IV as an indication of the fact that the W–O distances are of rather poor accuracy. Nevertheless, the values of v_w agree with the observations made for the DPTB_h 's (Table IV) and $\text{P}_8\text{W}_{12}\text{O}_{52}$ (9) and for $\text{P}_4\text{W}_{12}\text{O}_{44}$

and $\text{P}_4\text{W}_{16}\text{O}_{56}$ (10): the most distorted WO_6 octahedra are those having the most PO_4 neighbors and the highest oxidation state v_w .

The tilting of the m octahedra forming the chains is closely related to the configuration of the diphosphate groups. Four different cases have been observed, as shown in Fig. 2. In three of them (Figs. 2a–2c) the two P_2O_7 groups belonging to the same hexagonal tunnel are related to each other by a twofold axis, whereas in the fourth case (Fig. 2d) they are related through a 2_1 screw axis. Moreover the P_2O_7 groups located at both ends of a chain are sometimes oriented differently.

The rubidium bronzes $\text{Rb}_x(\text{P}_2\text{O}_4)_2(\text{WO}_3)_{2m}$ form an example where two different space groups have been observed. The low- m members ($m \leq 6$) are characterized by space group $A2/m$: in these members with narrow ReO_3 -type slabs, no displacement of the W atoms out of the plane located at $y = \frac{1}{4}$ can be observed. For the high- m members ($m > 6$) the W atoms are slightly displaced out of this plane, leading to $P2_1/c$ symmetry; nevertheless, the superstructure reflections are very weak, owing to the weak displacement of the atoms. In the same way, the cell parameters are related to the configuration of the octahedral chains. Two sorts of arrangements are observed depending on whether the configurations of the P_2O_7 groups at both ends of

TABLE IV
OXIDATION STATE (v) OF W ATOMS IN DPTB_h
 $m = 8$ MEMBERS VS THE NUMBER OF
 PO_4 TETRAHEDRA NEIGHBORS

	Number of P neighbors			
	0	0	1	2
$\text{Ba}_2\text{P}_8\text{W}_{32}\text{O}_{112}$	5.48	5.50	5.65	5.86
$\text{Rb}_{1.6}\text{P}_8\text{W}_{32}\text{O}_{112}$	5.55	5.67	5.69	5.89

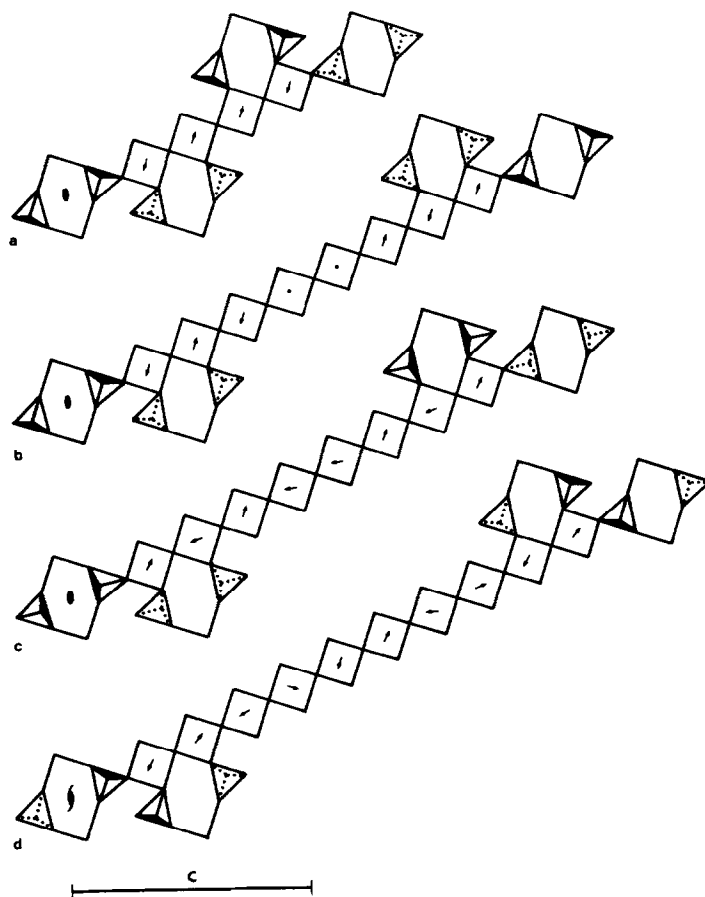


FIG. 2. The octahedral chains forming the ReO_3 -type slabs in the DPTB_h members: (a) $\text{Rb}_2\text{P}_8\text{W}_{16}\text{O}_{64}$, (b) $\text{Rb}_{1.6}\text{P}_8\text{W}_{32}\text{O}_{112}$, (c) $\text{Ba}_2\text{P}_8\text{W}_{32}\text{O}_{112}$, domain I, (d) $\text{KP}_8\text{W}_{40}\text{O}_{136}$. The schematic projections are oriented as for $\text{KP}_8\text{W}_{40}\text{O}_{136}$ in Ref. (4). The arrows show the tilting of the octahedra.

the chains are identical or different (Figs. 2a and 2b). In Fig. 2b the situation is identical at both ends of the chain (case of $m = 6$ and $m = 8$), but in Fig. 2a the situation is different (case of $m = 4$ and $m = 7$) because the P_2O_7 groups of the extremities of the chain are not located at the same level y . The correspondence between the two models can be understood by the effect of a $c/2$ gliding of a P_2O_4 slice with respect to the next P_2O_4 slice. Moreover, the tilting of the extreme octahedra of a chain must be compatible with the geometry of the P_2O_7 groups and that explains why in some cases, as for $m = 4$ (Fig. 2a), two succes-

sive octahedra in the chain are distorted in the same way or not tilted.

The potassium diphosphate bronzes, like the rubidium compounds, are characterized by rather weak superstructure reflections due to a weak displacement of the tungsten atoms. However, a different configuration of the octahedral chains can be observed. It is the case of the potassium DPTB_h 's corresponding to $m = 10$ (4). The octahedral chains of this bronze differ from those of the rubidium and barium compounds by the distribution of the P_2O_7 groups on the two sides of the hexagonal tunnel (Fig. 2d): they are related through a screw 2_1 axis and are

TABLE V
Ba₂P₈W₃₂O₁₁₂: POSITIONAL AND THERMAL
PARAMETERS WITH e.s.d.'s IN THE HYPOTHESIS OF
DOMAIN II (THE CENTER OF SYMMETRY IS AT 0 0 ½)

	x	y	z	B
Ba	0.4891(4)	½	0.4974(5)	$B_{eq} = 1.3(1)^a$
W(1)	0.25754(5)	0.2461(3)	0.35704(6)	$B_{eq} = 0.24(2)^a$
W(2)	0.35719(5)	0.2441(3)	0.60276(6)	$B_{eq} = 0.35(2)^a$
W(3)	0.14927(5)	0.2508(3)	0.61268(6)	$B_{eq} = 0.29(2)^a$
W(4)	0.05191(6)	0.2512(3)	0.37060(6)	$B_{eq} = 0.34(2)^a$
P	0.4353(4)	0.201(1)	0.3265(4)	0.26(8)
O(1)	0.261(1)	0.267(3)	0.606(1)	0.7(3)
O(2A)	0.267(3)	½	0.355(3)	1.4(7)
O(2B)	0.281(2)	0	0.383(3)	1.1(5)
O(3A)	0.051(2)	0	0.359(2)	0.8(4)
O(3B)	0.061(2)	½	0.390(3)	0.9(5)
O(4)	0.425(4)	0	0.317(4)	4.1(1) ^b
O(5)	0.4789(9)	0.280(2)	0.115(1)	0.2(2)
O(6)	0.163(1)	0.278(3)	0.370(1)	0.3(2)
O(7)	0.325(1)	0.280(3)	0.490(1)	0.6(3)
O(8A)	0.167(2)	½	0.126(2)	0.6(5)
O(8B)	0.149(3)	0	0.116(3)	1.6(6)
O(9A)	0.360(2)	0	0.607(2)	0.9(5)
O(9B)	0.387(2)	½	0.624(2)	0.7(4)
O(10)	0.051(1)	0.266(4)	0.124(1)	0.8(3)
O(11)	0.377(1)	0.284(3)	0.362(2)	1.3(4)
O(12)	0.215(1)	0.222(3)	0.244(1)	0.8(3)
O(13)	0.413(1)	0.290(3)	0.233(1)	0.5(3)
O(14)	0.102(1)	0.216(2)	0.495(1)	0.4(2)
O(15)	0	½	½	1.8(5)

^{a,b} Same remarks as in Table I.

not lying at the same level y . The consequence is an anisotropic coordination for the inserted ion, which is usual for K^+ .

In the case of the barium compound described here, the P_2O_7 groups are in a different orientation with respect to the tunnel axis (Fig. 2c). This feature is well marked: the bridging O(4) oxygen atoms on both sides of the tunnel are closer (4.88 Å) than in Rb structures (6.16 Å for $m = 8$). The tilting mode is shown in Fig. 2c. One can note, as in the other compounds, the existence of chains containing, when necessary, two consecutive octahedra with the same distortion.

It is worth noting that the thermal factor B of the bridging oxygen atom O(4) in the P_2O_7 group has a high value. Indeed the corresponding map of electron density shows an important elongation mainly in the [001] direction, suggesting a distribution

of O(4) on two sites, each of them being occupied at 50%. This second position of O(4) leads to the existence of a second model, with the same $A2/m$ space group, with correct interatomic distances if there is now a 2_1 axis in a hexagonal tunnel, and with a center of symmetry in a rhombic tunnel, contrary to the first model. A refinement of the new atomic positions (Table V) to $R = 0.049$ and $R_w = 0.060$ shows an appreciable difference for F only with odd k (and odd l) reflections. Then we have to consider in the same crystal the coexistence of two structural types as microdomains corresponding, in fact, to a different distribution of the P_2O_7 groups on both sides of the hexagonal tunnels. In the first domain (Table I), the distribution is similar to the one of $Rb_{1.6}P_8W_{32}O_{112}$ (I), where the diphosphate groups are related through the binary axis, so they lie at the same level y (Fig. 3a). Then, the inserted A ion is located at the level y where the P_2O_7 are missing and is eight coordinated. In the second domain, the P_2O_7 groups are related through a screw axis 2_1 (Fig. 3b) so they are staggered in the [010] direction as in $KP_8W_{40}O_{136}$ (4). Then the inserted A ion has two O(11) neighbors less but an additional neighbor which is the bridging O(4) atom of P_2O_7 . The geometry of the P_2O_7 group is changed due to the proximity of the A ion: it is certainly why in $Ba_2P_8W_{32}O_{112}$ one observes an extension of the O(4) electron density. This new position of O(4) leads to a correct Ba–O(4) distance of about 2.88 Å and to a tilting of the polyhedra in the second model which is similar to those of $KP_8W_{40}O_{136}$ (Fig. 2d). We tried to refine a model including the two domains by an elementary comparison of I_{obs} and $(KF_{C1}^2 + (1 - K)F_{C2}^2)$ for the odd k and l reflections, the even reflections being nearly unchanged. The improvement was poor with $R = 0.14$ (instead of 0.16) for a contribution of 22.5% for domain II. However, one can note the location of Ba^{2+} in the hexagonal

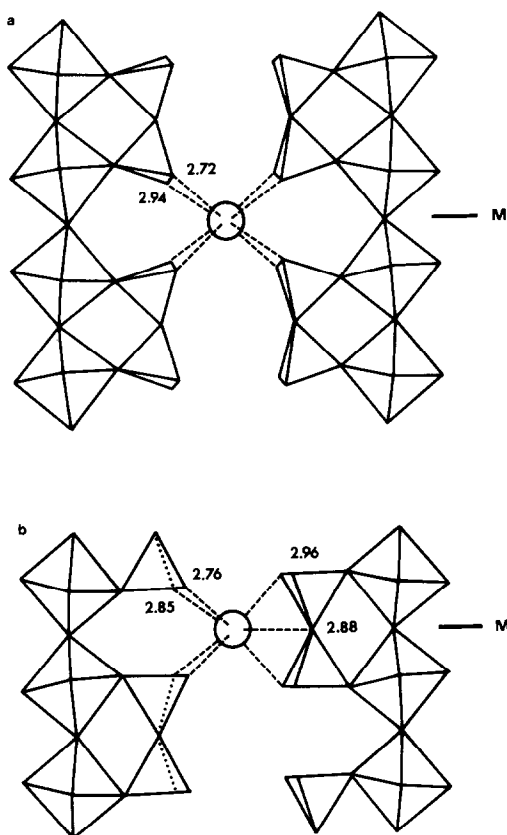


FIG. 3. Coordination of the Ba^{2+} ions for (a) domain I and (b) domain II.

tunnels at the level $y = \frac{1}{2}$ in domain I and $y = 0, \frac{1}{2}$ in domain II (then with an occupancy factor of 0.5). Any other position is unlikely because it brings about Ba–O distances shorter than 2.6 Å which is the minimum from the literature. The two assumed coordinations for Ba^{2+} appear in Fig. 3.

Conclusion

The structural study of the barium bronze $Ba_2P_8W_{32}O_{112}$, the eighth member of the series $A_x(P_2O_4)_2(WO_3)_{2m}$, shows the particular behavior of this oxide with respect to the univalent bronzes, especially by the fact that the superstructure reflections are so numerous that it is no longer possible to solve the structure in the classical subcell.

This phenomenon results from a greater displacement of the tungsten atoms from their ideal position, and is amplified by the fact that barium is much heavier than K and Rb, A ions of the previously studied compounds. The comparison of the chains of octahedra forming the ReO_3 -type slabs shows many differences dealing with cells and symmetries according to the nature of the A ions and the length of the chains. Thus, it seems that the Ba^{2+} ion, like K^+ , can adapt its size to two configurations of host framework in the field of $DPTB_h$'s. These configurations differ only in the distribution of the P_2O_7 groups and consequently in the tilting of the WO_6 polyhedra, but not in the relative distribution of W atoms, which remains nearly the same, very close to a plane according to a mirror symmetry. A possible interpretation of the anomalies observed in these structures deals with the existence of microdomains. A high-resolution electron microscopy study should bring more information about such models.

References

1. J. P. GIROULT, M. GOREAUD, PH. LABBÉ, AND B. RAVEAU, *Acta Crystallogr. Sect. B* **36**, 2570 (1980).
2. J. P. GIROULT, M. GOREAUD, PH. LABBÉ, AND B. RAVEAU, *Acta Crystallogr. Sect. B* **37**, 1163 (1981).
3. J. P. GIROULT, M. GOREAUD, PH. LABBÉ, AND B. RAVEAU, *Acta Crystallogr. Sect. B* **38**, 2342 (1982).
4. PH. LABBÉ, D. OUACHÉE, M. GOREAUD, AND B. RAVEAU, *J. Solid State Chem.* **50**, 163 (1983).
5. J. P. GIROULT, M. GOREAUD, PH. LABBÉ, AND B. RAVEAU, *Rev. Chim. Minér.* **20**, 829 (1983).
6. B. DOMENGES, M. HERVIEU, AND B. RAVEAU, *Acta Crystallogr. Sect. B* **40**, 249 (1984).
7. "International Tables for X-ray Crystallography," Vol. IV, p. 72. Kynoch Press, Birmingham (1974).
8. I. D. BROWN, in "Structure and Bonding in Crystals" (M. O'Keeffe and A. Navrotsky, Eds.), Vol. 2. Academic Press, New York (1981).
9. B. DOMENGES, N. K. MCGUIRE, AND M. O'KEEFFE, *J. Solid State Chem.* **56**, 94 (1985).
10. PH. LABBÉ, M. GOREAUD, AND B. RAVEAU, *J. Solid State Chem.* **61**, 324 (1986).